23rd International Conference on Renewable Energies and Power Quality (ICREPQ'25)
Tenerife (Spain), 25th to 27th June 2025
Renewable Energy and Power Quality Journal (RE&PQJ)
ISSN 2172-038 X, Volume No.23, September 2025

Influence of synchronous condensers on small isolated power systems with large amount of renewable energy. A case study of the Lanzarote-Fuerteventura power system

E.J. Medina Domínguez[1], J.F. Medina Padrón[2], J.M. De León Izquier[1]

[1] Renewable Energies Department, Canary Islands Institute of Technology (ITC)
C/Playa de Pozo Izquierdo s/n, Santa Lucía de Tirajana, Gran Canaria, 35119, Spain

[2] University of Las Palmas de Gran Canaria (ULPGC)
Campus de Tafira, Las Palmas de Gran Canaria, 35017, Spain

Abstract. This work studies the influence of synchronous condensers (SC) on small, isolated power systems with high levels of wind power, trying to quantify it using the rate of change of frequency ($RoCoF$), frequency nadir (f_{nadir}) and minimum voltage (U_{min}). Likewise, different values of the inertia constant of the SCs (H_{SC}) were studied.

To this end, a model of the Lanzarote-Fuerteventura electric power system is used, which has proven to be a useful representation of this type of power system. Two SCs have been modelled, connected to the power system. They were modelled taking into account the characteristics of one SC that will be installed in the Lanzarote-Fuerteventura power system, according to the electric transmission network planning.

A transient stability analysis was conducted, where the considered disturbance was the disconnection of generation power, simulated by the disconnection of a conventional generation unit.

Results suggest significant, positive effects on the system frequency and voltage values of the transmission buses throughout the small, isolated power system. In this way SCs could contribute to both the transient stability and the integration of the renewable energy, in small, isolated power systems

Key words. Small isolated power systems, synchronous condenser, wind generation, inertial response, transient stability.

1. Introduction

The deployment of renewable energy has seen a substantial increase worldwide in recent years, a development that has been influenced by both national and supranational policies.

The integration of large amounts of renewable energy into electric power systems brings with its issues, such as those related to its fluctuating nature, lower voltage control capability or lack of inertia contribution [1]. The greater the amount of renewable energy to be connected, the greater these issues will be.

Furthermore, within the context of small, isolated power systems, the aforementioned aspects are exacerbated. This is due to the fact that such systems present lower control capacities, lower total inertia, and weaker meshing when compared to mainland power systems.

In this context, the successful integration of large amounts of renewable energies into electric power systems requires actions that address both the inherent issues of renewable energies and those of small, isolated power systems.

One of the resources used is the synchronous condenser (SC), also known as synchronous compensator, synchronous capacitor or syncon. In essence, the SC is a synchronous machine connected to the network without prime mover or mechanical load.

The SC can generate or consume reactive power by controlling its excitation system. In addition, the SC contributes to the short circuit capacity of the power system and is also able to offer its rotational kinetic energy to improve the transient stability of the power system. [2-5].

The SC is not a new device, as it has been used for reactive power control since 1930 [3]. However, they are gaining importance in recent years due to their capabilities that favour the integration of renewable energies into the electric power systems.

So much so that European Network of Transmission System Operators for Electricity (ENTSO-E) [6] suggests

SC as a technological solution for inertia improvement in the power systems [7].

Nowadays, examples of installations or projects of SCs can be found in Australia, Spain, the United Kingdom and USA. [7].

As an example, in Spain it is planning to install several 100 MVA and 25 MVA SCs in the Balearic and Canary Islands power systems to improve their inertia, short-circuit power capacity and voltage control, according to the Spanish government's electric transmission network planning [8].

Several studies have been conducted in order to analyse the impact of SCs on the electric power system. In [9-12] the effect of SCs on mainland power systems has been analysed, taking into account renewable energies generation. The effects of SCs have also been studied in simplified models of electric power systems or in test models such as the two-area Kundur model or IEEE models, such as the IEEE39 test model [13-18]. In [19] the introduction of SC in a small isolated electric power system on an island with synchronous generation based on hydro generation and inverter-based resource (IBR) generation is studied.

The present study investigates the influence of SCs on small, isolated electric systems whose synchronous generation is based on diesel generation, and with a significant amount of wind generation. Besides, the electric power system under study is a real power system and it is made up of two other subsystems connected to each other by 132 kV and 66 kV submarine links. Furthermore, a range of inertia constant of SCs (H_{SC}) has been also investigated.

As a real example of this type of power system, the study is based on a model based on the current Lanzarote-Fuerteventura power system in year 2024. The Lanzarote - Fuerteventura power system is that of the Spanish islands of Lanzarote and Fuerteventura.

Two SCs have been considered and their modelling has been based on a real SC that is planned to be installed in the Lanzarote-Fuerteventura power system, according to the actual electric transmission network planning. In addition, the connection point of one of them is also the one specified by that planning.

The methodology used in the study is provided in section 2. Section 3 presents a description of the current Lanzarote-Fuerteventura power system. The modelling of both the Lanzarote-Fuerteventura power system and the SCs is addressed in section 4. Section 5 presents the results and discussion, while the main conclusions drawn from the analysis are summarized in section 6.

This study was developed in the framework of the research activities carried out within RESMAC project, Innovative and Strategic Renewable Energy Sources to drive the transition to climate neutrality in Macaronesia [20], funded by European Commission, Programme of Territorial Cooperation INTERREG VI-D Madeira-Azores-Canary Islands MAC 2021-2027, project number 1/MAC/2/2.2/0011.

2. Methodology

As indicated, this work consists of analysing the effects of SCs on small and isolated power systems, focuses on study of the transient stability.

The considered electric power system is the current power system of Lanzarote-Fuerteventura, which serves as a model for small, isolated power systems, in scenarios with wind power generation considering two equal SCs.

The effects are measured using the parameters of rate of change of frequency ($RoCoF$), frequency nadir (f_{nadir}) and minimum voltage (U_{min}). The $RoCoF$ is the derivative of the system frequency with respect to time. It indicates the system stability and how quickly frequency deviations occur. The f_{nadir} is defined as the lowest point that the system frequency reaches after a disturbance before it commences its recovery.

The modelling of the Lanzarote-Fuerteventura power system and the two SCs, as well as the transient stability analysis, were carried out using the PSS®Ev32 software [21].

The analysis is performed for the extreme power demand conditions during normal operation of the power system, which are off-peak and peak demand states.

In each demand state, a particular case has been considered in which 100 % of power demand is covered by conventional generation, hereinafter referred to as conv case. In another case, 30 % of power demand is supplied by wind generation, with the remaining 70 % being covered by conventional generation, hereinafter referred to as conv-wind case.

The SCs have been studied, one in the part of the power system on the island of Lanzarote (connected to the 132 kV busbar of the Tías substation) and the other in the part corresponding to the island of Fuerteventura (connected to the 132 kV busbar of the Jares substation), the latter according to the actual electric transmission network planning. Rated power of each SC is 25 MVA (±25 MVAr).

Different H_{SC} values have been considered due to its is significant SC characteristic. H_{SC} is the rotational kinetic energy stored in the rotating masses at rated speed divided by the rated apparent power of the SCs.

The values investigated range from 2.0 to 7.0 MWs/MVA, in steps of 0.5 MWs/MVA. This range is into typical H_{SC} values range of SCs with flywheel [22]. Therefore, a range of cases have been examined in which the SCs are distinguished exclusively by the value of their H_{SC}. Besides, these cases in which the SCs are connected for study are identical to the conv-wind cases. This allows for a direct observation of the effects of the SCs in cases

where wind power is generated in the power system. Thus, cases with connected SCs are referred to as conv-wind-SC cases in this paper.

The power system disturbance to analyse the influence of SCs is the conventional generation loss. This generation loss was simulated by the sudden loss of a generation unit belonging to one of the conventional power plants in the power system. Specifically, the disconnected generation unit is the Diesel 9 generator unit of the Punta Grande power plant. Table I presents the active power generated by this generation unit for each case, in addition to its percentage contribution to the total generated active power in the power system.

To establish each case, the corresponding technical-economic dispatches of the generation units were made while maintaining the corresponding spinning reserves.

The total wind power generated in each case is distributed among the different wind farms in proportion to their rated power. Likewise, the voltages setpoint of conventional generators for both studied demand states are consistent with real operational practices in the power system.

In order to observe more clearly the effects of SCs on the power system, the wind generation capabilities of active power control and reactive power/voltage control were disabled. This is consistent with the current operation of the Lanzarote-Fuerteventura power system. Despite the mandatory requirement for wind generation to be equipped with these capabilities [23], at present the active power frequency response capability by wind generation is not used.

3. Brief Description of the Studied Power System

The Lanzarote-Fuerteventura electric power system is located on the islands of Lanzarote and Fuerteventura, which are part of the Canary Islands archipelago, Spain.

The power system on the island of Lanzarote is connected to that on Fuerteventura by two submarine power cables, forming a single power system.

Each island has a conventional thermal power plant, Punta Grande power plant on the island of Lanzarote and Las Salinas on the island of Fuerteventura. Both plants have diesel and gas turbine generation units. Table II shows these conventional generation units and the total capacity of the power plants [24,25].

Table I. – Generated active power by Diesel 9 generation unit of the Punta Grande power plant.

Off-peak demand state		Peak demand state	
conv case	conv-wind case	conv case	conv-wind case
13.52 MW 11.55 %	13.52 MW 11.55 %	15.72 MW 6.11 %	15.72 MW 6.11 %
Percentage values referred to the total generated active power in the power system.			

The transmission network consists of 13 substations and power lines with two rated voltage levels, 66 kV and 132 kV.

As mentioned above, there are two transmission submarine power cables connecting the parts of the power system on each island. One of the submarine power cables has a nominal voltage of 66 kV and a capacity of 60 MVA, while the other has a nominal voltage of 132 kV and a capacity of 120 MVA.

There are also several generation substations to connect renewable generation units to the transmission network.

The current installed wind power capacity is 96.76 MW, but this value is expected to increase as more wind farms are installed in the near future. Table III presents the current wind farms, their respective rated active power and wind turbine technology.

The currently installed grid-connected solar photovoltaic capacity is approximately 55 MW [25].

In 2023, off-peak demand was 177.02 MW, while peak power demand reached 255.33 MW [26].

4. System Modelling

The modelling of the current Lanzarote - Fuerteventura electric power system in the year 2024 and the simulation have been carried out using the PSS®E v33.12.0 software [21].

Conventional and wind generation and the transmission network are specifically modelled. The distribution network and loads are represented together by lumped loads in the corresponding substations.

Each conventional generation unit has been modelled with its set-up transformer.

Transmission power lines are modelled using the π model without conductance. The power factor of the lumped loads is 0.9.

Table II. – Conventional generation in Lanzarote-Fuerteventura power system

PUNTA GRANDE GENERATION UNITS	CAPACITY (MVA)	LAS SALINAS GENERATION UNITS	CAPACITY (MVA)
Diesel 1	9.40	Diesel 1	5.40
Diesel 2	9.40	Diesel 2	5.40
Diesel 3	9.40	Diesel 3	6.30
Diesel 4	19.50	Diesel 4	9.40
Diesel 5	19.50	Diesel 5	9.40
Diesel 6	30.00	Diesel 6	30.00
Diesel 7	22.50	Diesel 7	22.50
Diesel 8	22.50	Diesel 8	22.50
Diesel 9	21.75	Diesel 9	22.50
Diesel 10	21.75	Gas 1	31.25
Diesel 11	22.50	Gas 2	48.00
Gas 1	31.25	Gas movil 1	16.75
Gas 2	46.88	Total	229.40
Total	286.00		

Table III. – Current wind farms in the Lanzarote-Fuerteventura power system

WIND FARM	WIND TURBINE TYPE	RATED ACTIVE POWER (MW)
Los Valles	Type 3	8.5
Punta Grande	Type 4	4.6
Arrecife	Type 4	9.2
Teguise	Type 4	9.2
CAAF Puerto del Rosario	Type 4	2.35
CAAF Corralejo	Type 3	1.7
Fuerteventura Renovable I	Type 4	4.7
Fuerteventura Renovable II	Type 4	4.7
Fuerteventura Renovable III	Type 4	2.35
Cañada de La Barca	Type 1	10.26
Aliso	Type 3	10
Puerto del Rosario	Type 3	29.2
Type 1: Squirrel cage induction generator (SCIG) wind turbine Type 3: Doubly-fed induction generator (DFIG) wind turbine Type 4: Full converter wind turbine		

The power transformers have been modelled as two-winding transformers, where the transversal parameters have been neglected.

Each wind farm was implemented as a single equivalent machine representing all its wind turbines.

As previously stated, the active power - frequency control and reactive power / voltage control capabilities of the wind farms were disabled to obtain more accurate results related to the effects of SCs on power system.

For the same purpose of achieving more accurate results regarding the effects of SCs, the lumped loads were considered constant in both active power and reactive power.

The SCs have been implemented connected to the transmission network, one on each island. Specifically, the SC corresponding to the island of Fuerteventura is modelled connected to the Jares 132 kV substation, as indicated in the Spanish government's electric transmission network planning [8]. The remaining one is connected to the 132 kV Tías substation on the island of Lanzarote. Set-up transformers have been modelled in order to establish a connection between the SCs and the 132 kV busbars of the substations previously referenced.

A simplified single-line diagram of the model of the Lanzarote-Fuerteventura power system with the studied SCs is shown in figure 1.

A. Conventional Generation

The diesel generation units are represented by:

- GENSAL (Salient pole generator model).
- DEGOV1 (Woodward diesel governor).
- SEXS (Simplified excitation system).

The models used for the modelling of the gas turbine generation units are as follows:

- GENROE (Round rotor generator model).
- GAST2A (Gas turbine model).
- ESDC1A (IEEE type DC1A excitation system).

These models are well-know and related information can be found in [27,28].

B. Squirrel cage induction generator wind turbine

The squirrel cage induction generator wind turbine (SCIG), also called type 1 wind turbine, is implemented by a generator model (WT1G1), a two-mass turbine model (WT12T1) and a pseudo-governor model (WT12A1) [27].

Normally, this type of wind turbine is equipped with a capacitor bank for power factor compensation. Therefore, a two-step capacitor bank was modelled for this type of wind turbine.

C. Doubly-fed induction generator wind turbine

As with SCIG wind turbine, modelling of the doubly-fed induction generator (DFIG) wind turbine (type 3) requires consideration of the mechanical components as this type of wind turbine has a direct connection between the stator winding of its generator and the grid.

Therefore, the models used to represent this type of wind turbine are as follows:

- REGCAU1 (REGC_A) (Renewable energy generator/converter model).
- REECAU1 (REEC_A) (Renewable energy electrical model).
- REPCAU1 (REPC_A) (Wind turbine plant controller model)
- WTDTAU1 (WTGT_A) (Wind turbine mechanical system model)
- WTARAU1 (WTGA_A) (Wind turbine aerodynamic model).
- WTPTAU1 (WTGP_A) (Wind turbine pitch control model).
- WTTQAU1 (WTGQ_A) (Generic torque controller for type 3 wind machines).

All of the aforementioned models are classified as constituting the second generation of renewable energy models [27,29].

D. Full converter wind turbine

The following models are utilised for the purpose of modelling the full converter wind turbine (type 4):

- REGCAU1 (REGC_A) (Renewable energy generator/converter model).
- REECAU1 (REEC_A) (Renewable energy electrical model).
- REPCAU1 (REPC_A) (Wind turbine plant controller model).

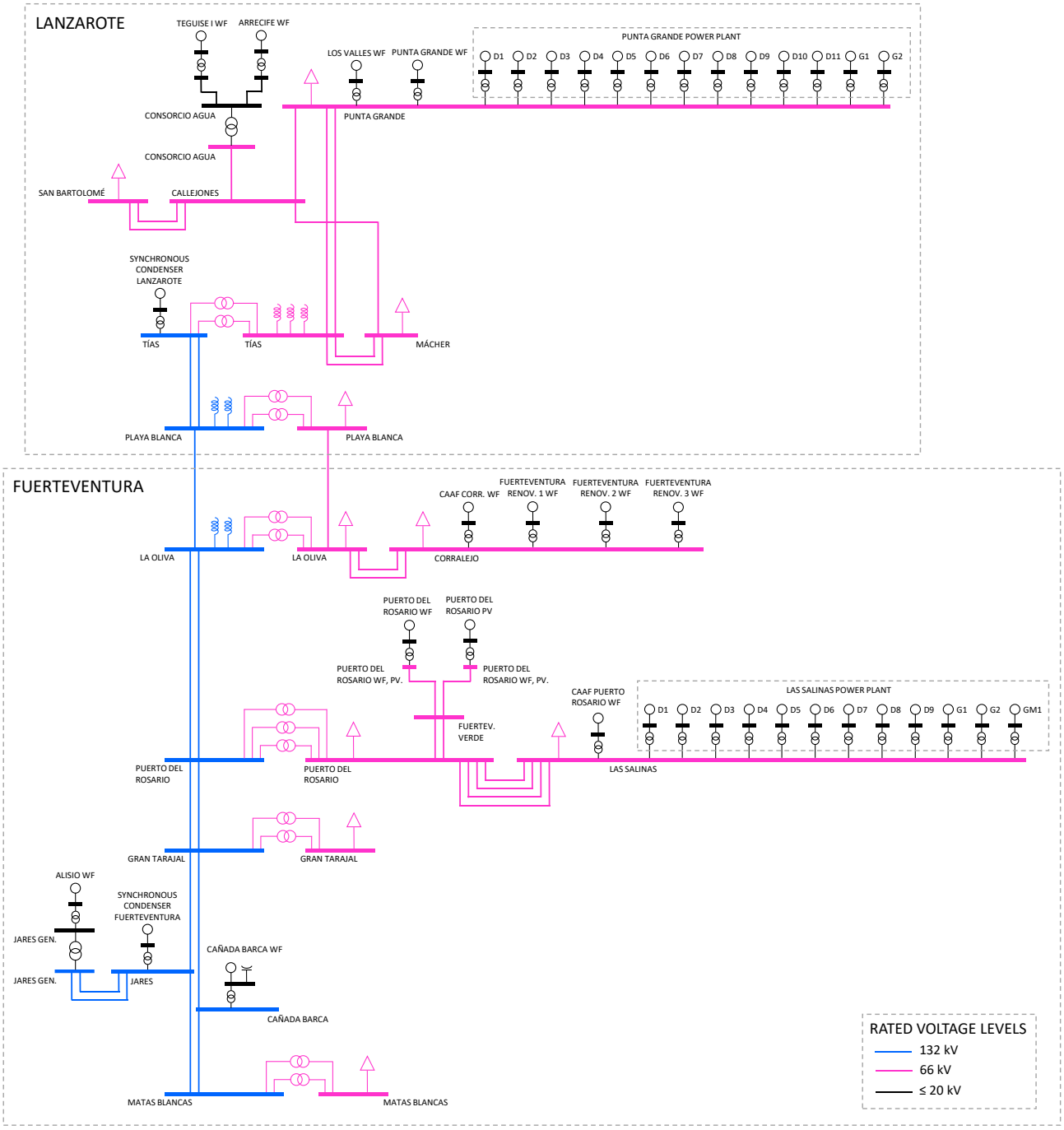

Fig. 1. Simplified single-line diagram of the model of the Lanzarote-Fuerteventura electric power system.

E. Protection relays

Undervoltage, overvoltage, underfrequency and overfrequency protections for both conventional and wind power generation have been represented, the models used being the VTGTPAT (Under/over voltage generator trip relay) and FRQTPAT (Under/over frequency generator trip relay) [27].

Adjusted values meet the current regulatory requirements [30,31].

F. Load Shedding Scheme

A load shedding scheme has been implemented in the power system model by using the LDSHBL (Underfrequency load shedding model) [27]. Three load shedding steps have been implemented for each lumped load. The setting values are the actual existing values [32].

G. Synchronous condenser

The two SCs have been modelled in an attempt to represent as closely as possible the one that will be installed in the Lanzarote-Fuerteventura power system in

the future according to the electric transmission network planning [8].

In this regard, the synchronous machine is expected to be a four-pole salient-pole machine with a rated power of 25 MVA (±25 MVAr) and a rated voltage of 11 kV. Moreover, the excitation system is considered to be brushless excitation system [33-35].

In view of the aforementioned points, the selection of the generator model GENSAL (Salient Pole Generator) and the excitation model ESAC6A (IEEE Type AC6A Excitation System) [27] has been made for representation of the SC.

5. Results and Discussion

The results obtained from the present study firstly indicate that in the event of a sudden disconnection of the Diesel 9 generator unit of the Punta Grande power plant, a decline in system frequency is observed, which then stabilises. This system frequency behaviour is well-known, and it can be seen in figure 2 that shows the system frequency time evolution for both the conv case and the conv-wind case.

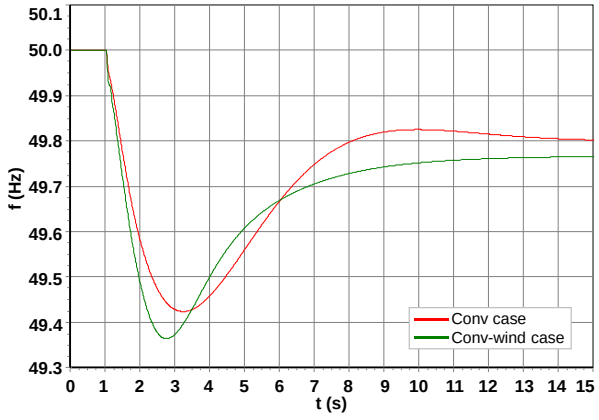

a)

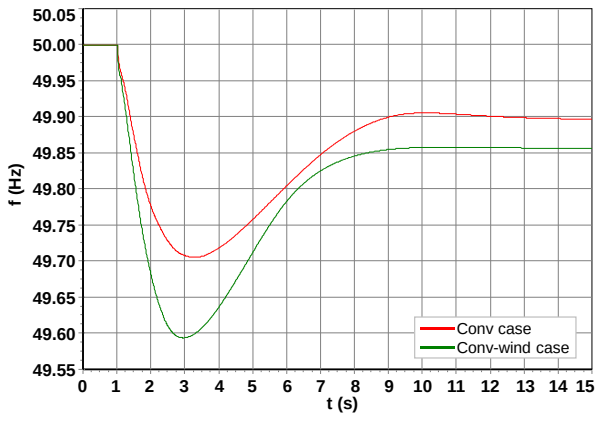

b)

Fig. 2. System frequency time evolution for a sudden disconnection of the Diesel 9 generator unit of Punta Grande power plant for conv case and conv-wind case: a) off-peak demand state; b) peak demand state.

This system frequency evolution is related to the behaviour of synchronous generators, since the power system under study is based mainly on these machines. Therefore, the swing equation of the synchronous machine (equation 1) [36] can be used to explain part of the frequency behaviour of the system.

$$\frac{H}{\pi f}\frac{d^2\delta}{dt^2} = P_a = P_m - P_e \quad (1)$$

where:
H: Inertia constant
f: System frequency
$\frac{d^2\delta}{dt^2}$: Rotor acceleration
P_a: Accelerating power
P_m: Mechanical power from prime mover
P_e: Electrical power.

In the event of disconnection of the Diesel 9 generator unit, the remaining generators immediately increase their electrical power output P_e. According to the swing equation, if P_e increases, a negative acceleration occurs, so the generators will start to slow down their rotor speeds. This is because the increased P_e is at the expense of their rotational kinetic energy. As the system frequency is directly related to the rotational speed of the generation units, a decrease in speed also leads to the observed decline in system frequency. Subsequently, due to the action of the speed governors, which cause the prime movers to increase their P_m, the system frequency stabilises.

Furthermore, a different system frequency behaviour between the conv case and the conv-wind case can be observed. The conv-wind case presents a more severe system frequency excursion, characterised by a higher value of $RoCoF$ (in absolute values) and lower f_{nadir}. This can be attributed to two key factors. Firstly, a lower total inertia constant of the power system (H_t) and secondly, a lower total active power frequency response capability of the power system in the conv-wind case. Lower values of H_t will result in larger system frequency excursions, according to the swing equation. As basically H_t is provided by conventional generators, the lower H_t is due to the fact that fewer conventional generation units are connected, as part of the demand is covered by wind generation. Table IV presents the H_t in both cases.

In addition, it is expected that increasing the amount of connected wind generation will result in lower H_t values, for the reason mentioned above [37].

The voltages of the transmission buses throughout the small, isolated power system exhibit the typical effects caused by a reduction in generation. After the disconnection of the Diesel 9 generation unit, which was injecting reactive power, the voltages initially dropped followed by subsequent recovery (figure 3). A greater drop in voltage is observed in the conv-wind case given that, with fewer conventional generation units connected, the overall capacity for reactive power/voltage control in the power system is lower.

Table IV. - Total inertia constant of the power system provided from conventional generation units in the conv case and the conv-wind case.

Off-peak demand state		Peak demand state	
conv case	conv-wind case	conv case	conv-wind case
6.74	5.18	13.73	9.63
In MWs/MVA S_{base}= 100 MVA			

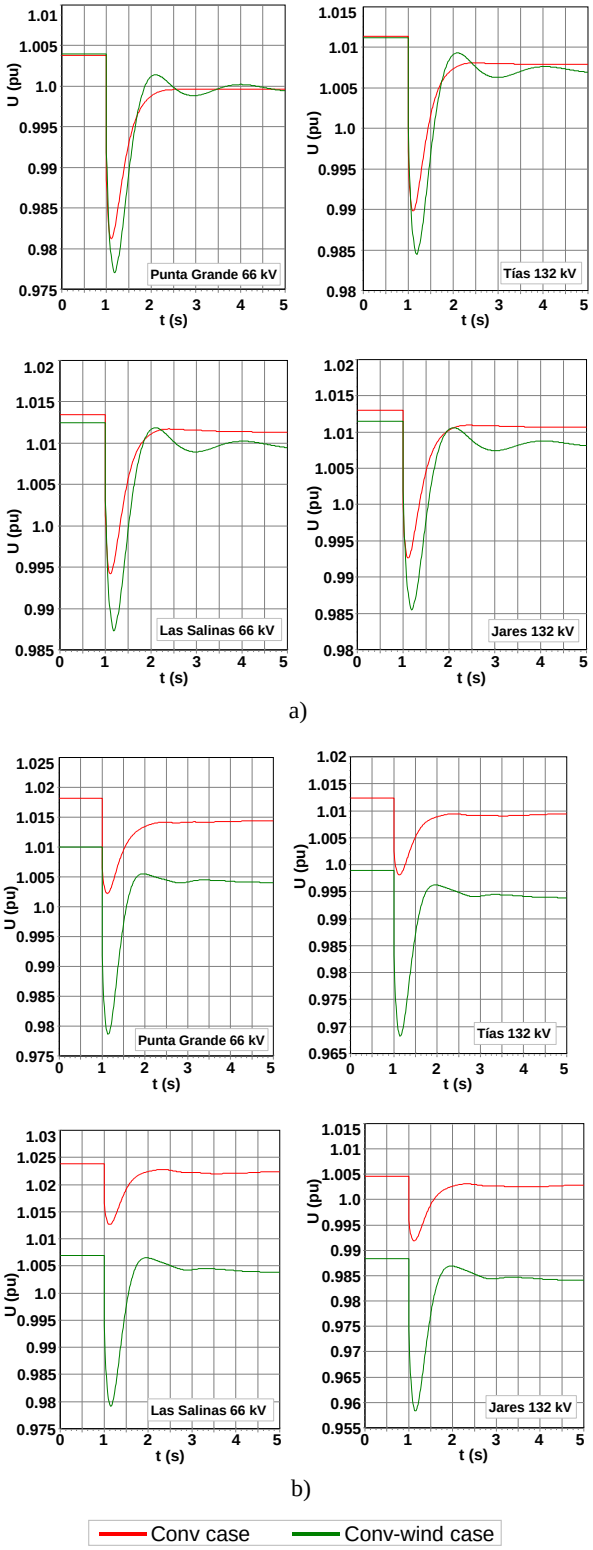

Fig. 3. Voltage time evolution for a sudden disconnection of the Diesel 9 generator unit of Punta Grande power plant for conv case and conv-wind case: a) off-peak demand state; b) peak demand state.

In the case where the SCs are connected (conv-wind-SC case) with a H_{SC} value of 2 MWs/MVA, the system frequency excursions are in general terms smaller compared to the conv-wind case. This can be seen in figure 4.

These differences between the system frequency excursions can be quantified by means of the $RoCoF$ and the f_{nadir}. Table V presents the corresponding values for each case.

Compared to the conv-wind case, the $RoCoF$ of the conv-wind-SC case is 0.14 and 0.05 Hz/s lower (in absolute values) for the off-peak and peak demand states respectively.

The general, smaller excursions of the system frequency in conv-wind-SC case are caused by the active power injected by the SCs. When disconnection of the generation unit takes place, SCs inject active power into the network from its rotational kinetic energy. This is illustrated in figure 5, which presents the active power injected by the two SCs when the conventional generator is disconnected in one of the studied cases.

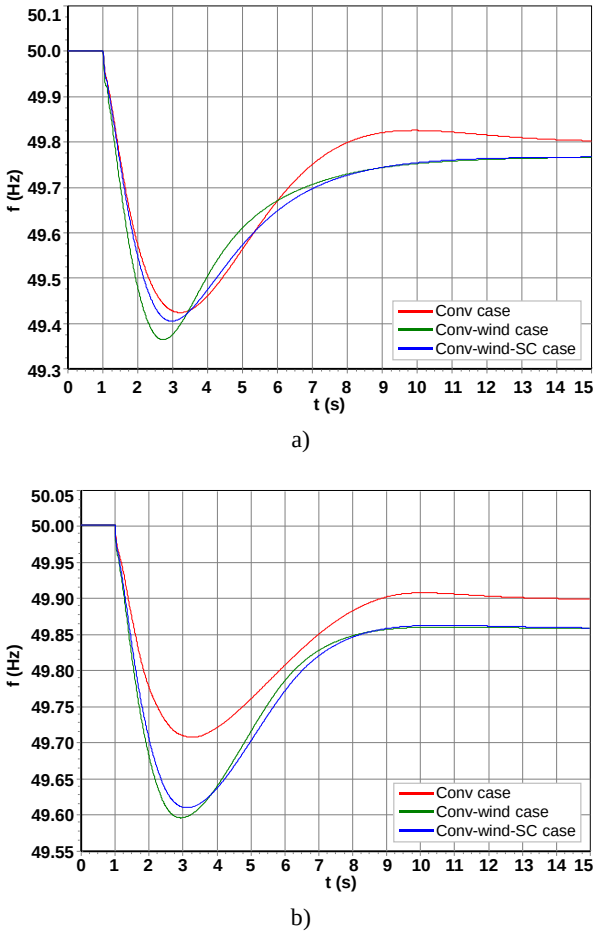

Fig. 4. System frequency time evolution for a sudden disconnection of the Diesel 9 generator unit of Punta Grande power plant for conv case, conv-wind case and conv-wind-SC case (H_{SC}= 2 MWs/MVA): a) off-peak demand state; b) peak demand state.

Table V. - $RoCoF$ and f_{nadir} in conv case, conv-wind case and conv-wind-SC case (H_{SC}= 2.0 MWs/MVA).

	Off-peak demand state			Peak demand state		
	conv case	conv-wind case	conv-wind-SC case	conv case	conv-wind case	conv-wind-SC case
$RoCoF$ (Hz/s)	-0.59	-0.76	-0.62	-0.35	-0.44	-0.39
f_{nadir} (Hz)	49.42	49.36	49.41	49.71	49.59	49.61

However, as it is also depicted in figure 5, from instant 2.92 s, the SCs start consuming active power from the network to restore their rotational kinetic energy. This active power consumption induces a delay in system frequency recovery (see figure 4 for the period of 3.5 – 8.5 s)

These power interchanges between SCs and the network is related to the equation 1. Since SCs lack prime mover, P_m does not exist, thus, the power injected into the network or consumed from it comes from the modification of their rotational kinetic energy, as mentioned and is called inertial response. A more detailed explanation of the involved synchronous machine internal phenomena can be found in [38,39].

The effect of the SCs under study on the voltage in the power system is also significant. As illustrated in figure 6, the obtained U_{min} values throughout the power system are increased due to the generation of reactive power by SCs.

In comparison with the conv-wind case, the U_{min} values obtained in the conv-wind-SC case for the 66 kV and 132 kV buses of the transmission network are on average 0.025 pu (1.65 kV) and 0.021 pu (2.77 kV) higher respectively. The values of U_{min} for all the studied cases are shown in the Appendix.

This is due to the fact that the SCs help to support voltage in the event of the loss of conventional generation unit by injecting reactive power, as it can be seen in figure 7.

As previously referenced, a values range of H_{SC} was also considered, with this range being between 2.0 and 7.0 MWs/MVA, in steps of 0.5 MWs/MVA. Thus, different conv-wind-SC cases with these H_{SC} values were studied.

A comparison of the time evolution of the system frequency indicates a lower $RoCoF$ (in absolute values) and a higher f_{nadir} for higher H_{SC} values, as can be seen in figure 8.

Taking conv-wind case as reference, the system frequency excursion for conv-wind-SC case with H_{SC}= 7.0 MWs/MVA exhibit a $RoCoF$ of 0.22 and 0.09 Hz/s lower for off-peak and peak demand states respectively (in absolute values). The values of both $RoCoF$ and f_{nadir} for all the studied cases are given in the Appendix.

It can also be observed that the time at which f_{nadir} occurs increases as H_{SC} increases.

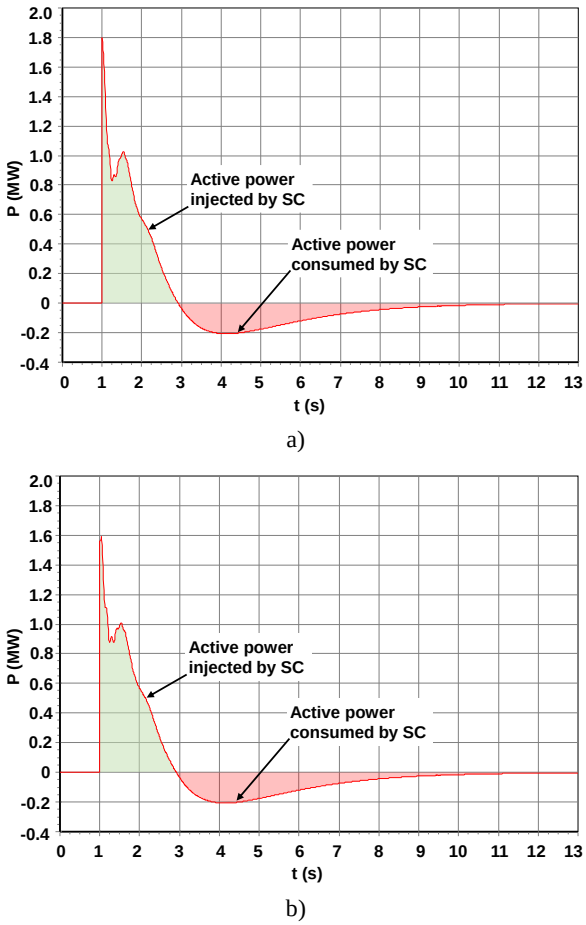

Fig. 5. Active power of the SCs (H_{SC}=2.0 MWs/MVA) connected in a) Tías substation (Lanzarote) and in b) Jares substation (Fuerteventura) for a sudden disconnection of the Diesel 9 generator unit of Punta Grande power plant, off-peak demand state.

As seen previously, the SCs inject active power by their inertial response in the event of a loss of generation. Since H_{SC} is the rotational kinetic energy stored in the rotating masses at rated speed divided by the rated apparent power of the SCs, it can thus be deduced that a higher H_{SC} value corresponds to an increase of the SCs inertial response capacity, thereby achieving the aforementioned smaller frequency excursions.

It can also be seen that the obtained reduction in $RoCoF$ values (in absolute terms) is not proportional to the increase in H_{SC}. This indicates the possible existence of a technical economic limit to the value of H_{SC}, beyond which its increase is not justified.

A noticeable delay in the system frequency recovery is also observed. This delay exhibits an increase as the studied value of H_{SC} is higher. It is also illustrated in figure 8, taking place in the period of time between approximately 3.5 s and 10 s. As previously mentioned, this delay in the recovery of the system frequency is the result of the active power consumption of the SCs. This must be taken into account, as it could lead to unacceptable negative effects on the system frequency.

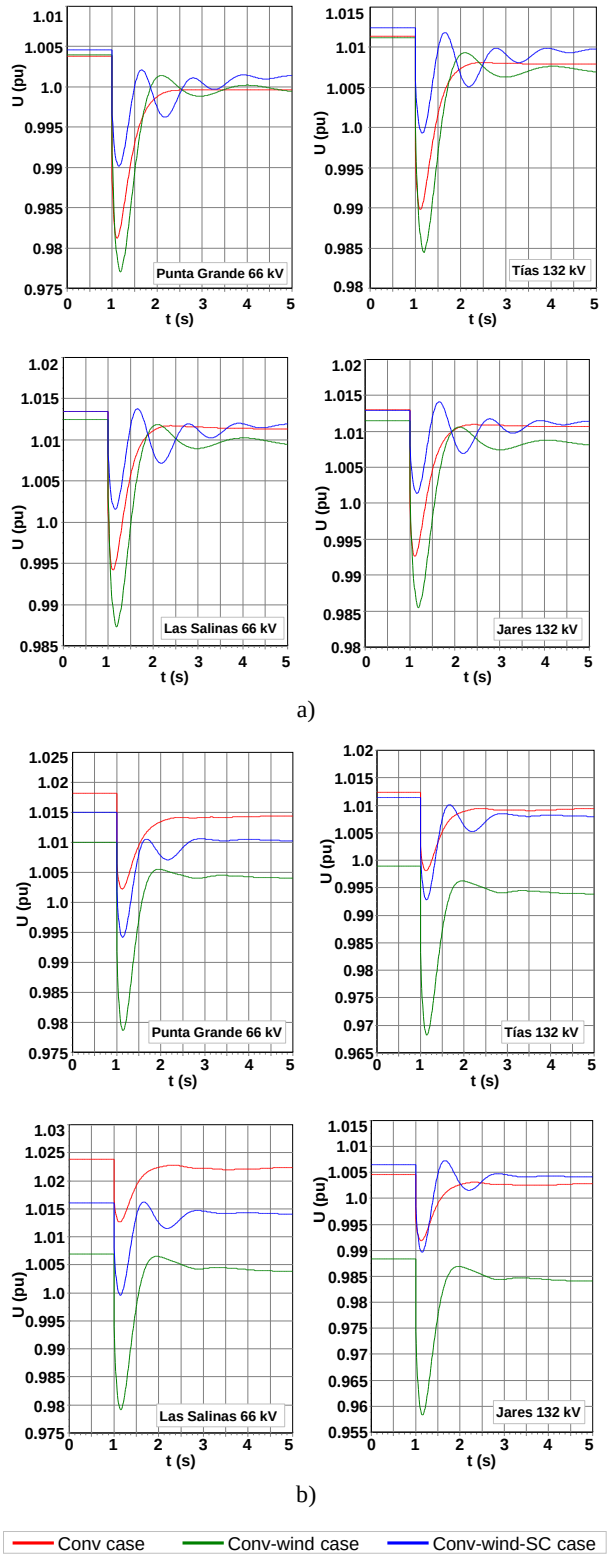

Fig. 6. Voltage time evolution for a sudden disconnection of the Diesel 9 generator unit of Punta Grande power plant for conv case, conv-wind case and conv-wind-SC (H_{SC}=2.0 MWs/MVA): a) off-peak demand state; b) peak demand state.

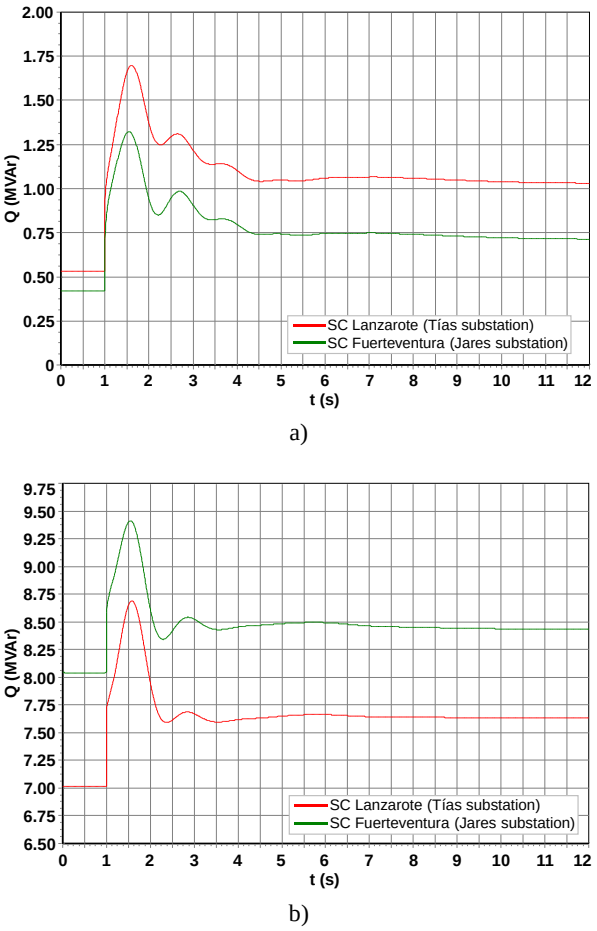

Fig. 7. Reactive power of the SCs (H_{SC}=2.0 MWs/MVA) in conv-wind-SC case for a sudden disconnection of the Diesel 9 generator unit of Punta Grande power plant in: a) off-peak demand state; b) peak demand state.

As might have been anticipated, the results showed that the different H_{SC} values considered did not have significantly different effects on power system voltages. This is because H_{SC} has no direct relationship with the SCs capacity to generate or consume reactive power. The values of U_{min} for each case can be found in the appendix.

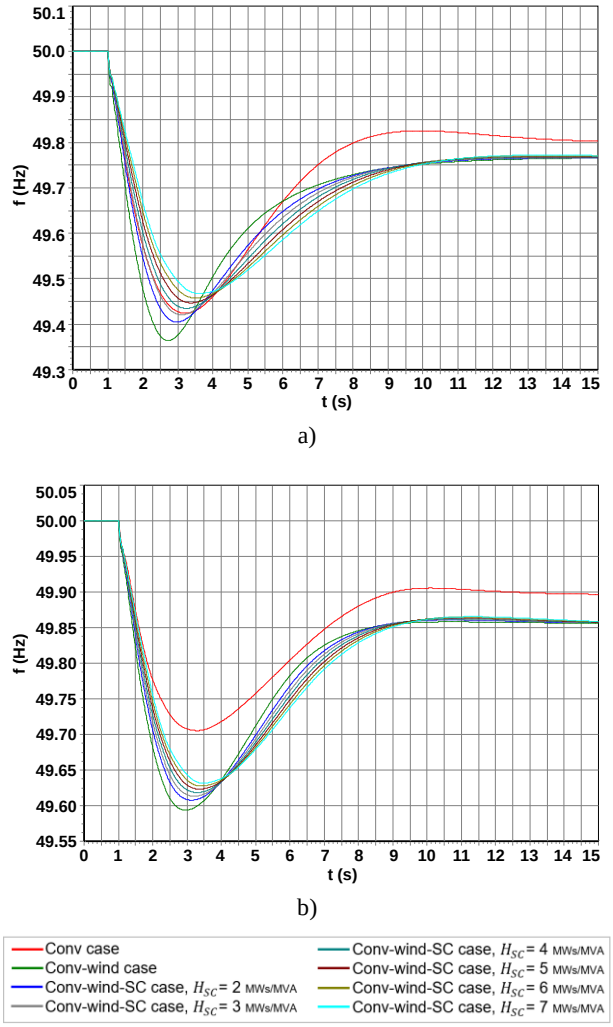

Fig. 8. System frequency time evolution for a sudden disconnection of the Diesel 9 generator unit of Punta Grande power plant for conv case, conv-wind case and conv-wind-SC cases: a) off-peak demand state; b) peak demand state.

6. Conclusions

This study investigates the impact of synchronous condensers (SC) on small, isolated power systems based mainly on diesel generation with large amount of renewable energy, more specifically wind power.

To do so, a model of the Lanzarote-Fuerteventura electric power system is used, which serves as a representative example of a small, isolated power system. In addition, two SCs are modelled, similar to one that will be installed in near future in the Lanzarote-Fuerteventura power system according to the real electric transmission network planning. Furthermore, the present study investigated the effects of different values of the inertia constant of the SCs (H_{SC}), ranging from 2.0 to 7.0 MWs/MVA.

To analyse the impact of SCs, a conventional generation loss disturbance is considered, which was simulated by the sudden loss of a generation unit belonging to a conventional power plant in the power system.

A loss of generation in a power system generally leads to a system frequency excursion, which is characterised by an initial drop. The findings indicate that in a scenario characterised by a high wind power penetration in a small, isolated power system, a positive reduction in system frequency excursions can be expected if SCs are in operation. In this sense, the SCs cause a reduction of the rate of change of frequency ($RoCoF$) (in absolute values) and an increase of the system frequency nadir (f_{nadir}). As an example of SCs with H_{SC}= 2.0 MWs/MVA in operation, the $RoCoF$ is reduced by 0.14 and 0.05 Hz/s (in absolute values) for the off-peak and peak demand states of the power system respectively. This reduction in system frequency excursions is due to the active power injected by the SCs through their inertial response when a conventional generation is lost.

A disconnection of a conventional generator unit that produce reactive power commonly results in a voltage drop. The results suggest a positive influence of the SCs on the voltage of the transmission buses throughout the power system when generation unit loss occurs. In this respect, it has been determined that the minimum voltage (U_{min}) obtained are on average 0.025 pu and 0.021 pu greater for the 66 kV and 132 kV buses of the transmission network, respectively. This is due to the reactive power generation/consumption capacity of the SCs, which collaborate in voltage support, and can be observed for all buses of the transmission network of this type of electric system.

The study also demonstrates an evident influence of the H_{SC} value of the SCs on the temporal evolution of the frequency of the small, isolated power system. An increase in the studied H_{SC} value leads a decrease in the $RoCoF$ and an increase in the f_{nadir}. For the highest considered value of H_{SC}, which is 7.0 MWs/MVA, the $RoCoF$ is reduced by 0.22 and 0.09 Hz/s for off-peak and peak demand states respectively. This is due to the inertial response of the SCs being greater as a result of a higher H_{SC} values.

It is noted that although the introduction of SCs with higher H_{SC} values leads to lower $RoCoF$ values (in absolute terms), the decrease in these $RoCoF$ values is not proportional to the increase in the H_{SC} value. This finding suggests the existence of a optimal value for H_{SC}, beyond which an increase in its value may not be techno-economic justifiable.

Despite these positive findings regarding the system frequency, a certain delay in its recovery is also observed for higher values of H_{SC}, caused by the active power consumption of the SCs as part of their inertial response. This should be considered, as it may lead to a significant negative impact on system frequency.

It is observed that the voltage of the transmission buses remains significantly unaffected by varying H_{SC} values.

In consideration of the results obtained for small, isolated electric power systems with a high level of wind power integration, it is demonstrated that SCs are elements that

contribute to the mitigation of system frequency events such as the one in the study. Furthermore, SCs are able to contribute to the support of the voltage throughout of the small, isolated power systems. These results indicate that SCs could contribute to the improvement of reliability and stability of the small, isolated power systems integrating renewable energy.

Therefore, SCs could be considered for increasing the integration of renewable energy into small, isolated power systems, although further research is needed on some aspects such as, for example, optimal rated power, optimal value of H_{SC}, most suitable location and behaviour of SCs under other disturbance conditions.

As a practical recommendation, the evaluation of a possible decrease in the total inertia of the electric power system and in its overall voltage/reactive power control capacity should be carried out in cases of large additions of renewable power replacing conventional synchronous generation. Should the evaluation indicate a substantial decrease, it would be necessary to increase them, with the addition of SCs serving to minimise their impact. This evaluation could be a part of the modern electric power systems growth plans.

Acknowledgement

This study was developed in the framework of the research activities carried out within RESMAC project, Innovative and Strategic Renewable Energy Sources to drive the transition to climate neutrality in Macaronesia [20], funded by European Commission, Programme of Territorial Cooperation INTERREG VI-D Madeira-Azores-Canary Islands MAC 2021-2027, project number 1/MAC/2/2.2/0011.

The authors would like to thank the Renewable Energies Department of the Canary Islands Institute of Technology (ITC) for its special support.

References

[1] E. J. Medina Domínguez, "Análisis de algunos aspectos técnicos relacionados con la integración de energías renovables en sistemas eléctricos pequeños y aislados," Ph.D. dissertation, Instituto Universitario de Sistemas Inteligentes y Aplicaciones Numéricas en Ingeniería, Universidad de Las Palmas de Gran Canaria. Las Palmas de Gran Canaria. Spain, 2016. [Online]. Available: http://hdl.handle.net/10553/18399.

[2] O. I. Elgerd, *Electric Energy Systems Theory: An Introduction*, 2nd ed. New York, NY, USA: McGraw-Hill, 1982.

[3] P. Kundur, *Power System Stability and Control*, New York, NY, USA: McGraw-Hill, 1994.

[4] M. Cortes Cherta, *Curso Moderno de Máquinas Eléctricas Rotativas. Tomo IV: Máquinas Síncronas y Motores de C.A. de Colector*, Barcelona, España: Editores Técnicos Asociados, 1994.

[5] P. E. Marken, A. C. Depoian, J. Skliutas, and M. Verrier, "Modern Synchronous Condenser Performance Considerations," in *2011 IEEE Power and Energy Society General Meeting*, Detroit, MI, USA, 2011, pp. 1–5. DOI: 10.1109/PES.2011.6039011.

[6] European Network of Transmission System Operators for Electricity (ENTSO-E). [Online]. Available: https://www.entsoe.eu [Accessed: Jan. 30, 2025].

[7] ENTSO-E, "Inertia and Rate of Change of Frequency (RoCoF)", Belgium, ENTSO-E, Report, v17, SPD – Inertia TF, 2020, [Online]. Available: https://eepublicdownloads.entsoe.eu/clean-documents/SOC%20documents/Inertia%20and%20RoCoF_v17_clean.pdf [Accessed: 31-Jan-2025].

[8] Ministerio para la Transición Ecológica y el Reto Demográfico, Gobierno de España, *Plan de Desarrollo de la Red de Transporte de Energía Eléctrica 2021-2026*, 2021. [Online]. Available: https://www6.serviciosmin.gob.es/Aplicaciones/Planificacion/PLAN_DESARROLLO_RdT_H2026_COMPLETO.pdf. [Accessed: 17-Jan-2025].

[9] H. T. Nguyen, G. Yang, A. H. Nielsen, and P. H. Jensen, "Frequency stability improvement of low inertia systems using synchronous condensers," in *Proc. 2016 IEEE Int. Conf. Smart Grid Commun. (SmartGridComm)*, Sydney, NSW, Australia, 2016, pp. 650-655, DOI: 10.1109/SmartGridComm.2016.7778835.

[10] N.-A. Masood, N. Modi, and R. Yan, "Low inertia power systems: Frequency response challenges and a possible solution," in *Proc. 2016 Australas. Univ. Power Eng. Conf. (AUPEC)*, Brisbane, QLD, Australia, 2016, pp. 1-6, DOI: 10.1109/AUPEC.2016.7749335.

[11] M. N. Haque Shazon, H. M. Ahmed, N.-A. Masood, and F. Hasan, "Supplementary inertial support in renewable integrated networks: Potential of synchronous condenser and energy storage," in *Proc. 2021 IEEE PES Innovative Smart Grid Technol. Europe (ISGT Europe)*, Espoo, Finland, 2021, pp. 1-5, DOI: 10.1109/ISGTEurope52324.2021.9640010.

[12] G. Zhou *et al.*, "Synchronous condenser applications: Under significant resource portfolio changes," *IEEE Power Energy Mag.*, vol. 17, no. 4, pp. 35-46, July-Aug. 2019, DOI: 10.1109/MPE.2019.2909005.

[13] Glaninger-Katschnig, "Contribution of synchronous condensers for the energy transition," *e & i Elektrotechnik und Informationstechnik*, vol. 130, no. 1, pp. 28-32, Feb. 2013, DOI: 10.1007/s00502-013-0119-3.

[14] A. Youssef, W. M. Hamanah, M. Zaery, and M. Abido, "Frequency stability enhancement using synchronous condenser and synthetic inertia in wind-dominated power grids: A case study," in *Proc. 2023 IEEE Int. Conf. Energy Technol. Future Grids (ETFG)*,

Wollongong, Australia, 2023, pp. 1-6, DOI: 10.1109/ETFG55873.2023.10407887.

[15] M. I. Pereira y C. Moreira, "Improving stability of reduced inertia transmission systems," in *Proc. 2024 IEEE 22nd Mediterr. Electrotechnical Conf. (MELECON)*, Porto, Portugal, 2024, pp. 443-448, DOI: 10.1109/MELECON56669.2024.10608674.

[16] E. Fouladi, A. Mehrizi-Sani, and B. Bahrani, "Optimal planning of synchronous condensers considering the impact of inverter-based resources," in *Proc. 2024 IEEE Energy Conversion Congr. Exposition (ECCE)*, Phoenix, AZ, USA, 2024, pp. 1265-1270, DOI: 10.1109/ECCE55643.2024.10861081.

[17] K. Xv, J. Jia, B. Xie, N. Yang, R. Wang, and Y. Xie, "Power grid inertia promotion strategy considering synchronous condenser support," in *Proc. 2023 6th Int. Conf. Energy, Electr. Power Eng. (CEEPE)*, Guangzhou, China, 2023, pp. 672-677, DOI: 10.1109/CEEPE58418.2023.10166024.

[18] S. Hadavi, N. Mohammed, A. Mehrizi-Sani, and B. Bahrani, "Quantifying stability in inverter-based weak grids in the presence of synchronous condensers," *IEEE Open Access J. Power Energy*, vol. 11, pp. 314-324, 2024, DOI: 10.1109/OAJPE.2024.3428365.

[19] F. Fernandes, J. Peças Lopes, and C. Moreira, "Combining batteries and synchronous condensers: the case study of Madeira island," in *Proc. 8th Int. Hybrid Power Plants & Syst. Workshop (HYB 2024), Hybrid Conf.*, Azores, Portugal, 2024, pp. 58-64, DOI: 10.1049/icp.2024.1819.

[20] *Innovative and Strategic Renewable Energy Sources to Drive the Transition to Climate Neutrality in Macaronesia (RESMAC Project)*. [Online]. Available: https://resmacproject.com

[21] *PSS®E version 33.12.0.* (2018). Siemens Industry, Inc., Siemens Power Technologies International. Accessed: Jan. 31, 2025. [Online]. Available: https://www.siemens.com/global/en/products/energy/grid-software/planning/pss-software/pss-e.html

[22] CIGRE, "Guide on the assessment, specification and design of synchronous condenser for power system with predominance of low or zero inertia generators", CIGRE, Technical brochure, ref. 885, ISBN 978-2-85873-590-7, 2022, [Online]. Available: https://www.e-cigre.org/publications/detail/885-guide-on-the-assessment-specification-and-design-of-synchronous-condenser-for-power-system-with-predominance-of-low-or-zero-inertia-generators.html [Accessed: 16-Jan-2025].

[23] España, "Resolución de 1 de febrero de 2018, de la Secretaría de Estado de Energía," *Boletín Oficial del Estado*, no. 42, 16-Feb-2018. [Online]. Available: https://www.boe.es/eli/es/res/2018/02/01/(3). [Accessed: 03-Oct-2024].

[24] Ministerio para la Transición Ecológica y el Reto Demográfico, Gobierno de España, *Registro Administrativo de Instalaciones de Producción de Energía Eléctrica*. [Online]. Available: https://www.miteco.gob.es/es/energia/energia-electrica/electricidad/regimen-ordinario/registro-instalaciones.html. [Accessed: 09-Oct-2024].

[25] Consejería de Transición Ecológica y Energía, Gobierno de Canarias, *Anuario Energético de Canarias 2022*. [Online]. Available: https://www.gobiernodecanarias.org/energia/descargas/SDE/Portal/Publicaciones/AnuarioEnergeticodeCanarias_2022.pdf. [Accessed: 18-Jan-2025].

[26] Red Eléctrica, esios. [Online]. Available: https://www.esios.ree.es

[27] Siemens Industry, Inc., Siemens Power Technologies International, *Model Library PSS®E 33.12.0*. (2018).

[28] The Institute of Electrical and Electronics Engineers, Inc., *IEEE Recommended Practice for Excitation System Models for Power System Stability Studies*, New York, USA, 2016. ISBN 978-1-5044-0855-4.

[29] Electric Power Research Institute (EPRI), *Model User Guide for Generic Renewable Energy System Models*, Palo Alto, CA, USA, 2023. [Online]. Available: https://www.epri.com/research/products/000000003002027129. [Accessed: 18-Jan-2025].

[30] Canarias, "Decreto 6/2015, 30 enero," *Boletín Oficial de Canarias*, no. 26, 12-Feb-2015. [Online]. Available: https://www.gobiernodecanarias.org/boc/2015/029/002.html. [Accessed: 05-Jan-2025].

[31] Red Eléctrica, EDistribución Redes Digitales SL, *Acuerdo de Condiciones y Ajustes de Relés en Redes Radiales a Tensión Inferior a 66 kV en los Sistemas Eléctricos de los Territorios no Peninsulares*, 2024. [Online]. Available: https://www.ree.es/sites/default/files/2024-05/Acuerdo_Condiciones_Ajustes_Reles_Redes_Radiales.pdf. [Accessed: 05-Jan-2025].

[32] España, "Resolución de 16 de enero de 2024, de la Dirección General de Política Energética y Minas, por la que se aprueban los planes de deslastre automático de cargas de aplicación en los sistemas eléctricos de los territorios no peninsulares balear y canario," *Boletín Oficial del Estado*, no. 27, 31-Jan-2024. [Online]. Available: https://www.boe.es/diario_boe/txt.php?id=BOE-A-2024-1858. [Accessed: 05-Jan-2025].

[33] Red Eléctrica, *Proyecto Técnico Administrativo. Ampliación Subestación Jares 132 kV y Compensador Síncrono*, 2023.

[34] ABB, “ABB's integrated technology will stabilize the power grid as Spanish islands transition to green energy,” *Group Press Release*, Zürich, Switzerland, 05-Jun-2024. [Online]. Available: https://new.abb.com/news/detail/116318/abbs-integrated-technology-will-stabilize-the-power-grid-as-spanish-islands-transition-to-green-energy. [Accessed: 27-Sep-2024].

[35] ABB, *Deploying Synchronous Condensers to Provide Distributed Power Grid Support: ABB White Paper*, 2020. [Online]. Available: https://library.e.abb.com/public/945a0742f0a04e47a3577226c28784ee/White_paper_Distributed_grid_support_9AKK108141_RevA_EN.pdf. [Accessed: 03-Jan-2025].

[36] J. J. Grainger and W. D. Stevenson, *Power Systems Analysis*, New York, NY, USA: McGraw-Hill, 1994.

[37] E. J. Medina Domínguez and J. F. Medina Padrón, “Critical Clearing Time and Wind Power in Small Isolated Power Systems Considering Inertia Emulation,” *Energies*, vol. 8, no. 11, pp. 12669–12684, 2015. DOI: 10.3390/en81112334.

[38] F. Gonzalez-Longatt, J. M. Roldan-Fernandez, H. R. Chamorro, S. Arnaltes, and J. L. Rodriguez-Amenedo, “Investigation of Inertia Response and Rate of Change of Frequency in Low Rotational Inertial Scenario of Synchronous Dominated System,” *Electronics*, vol. 10, no. 18, p. 2288, 2021. DOI: 10.3390/electronics10182288.

[39] Y. Huang, Y. Wang, C. Li, H. Zhao, and Q. Wu, “Physics Insight of the Inertia of Power Systems and Methods to Provide Inertial Response,” *CSEE Journal of Power and Energy Systems*, vol. 8, no. 2, pp. 559–568, Mar. 2022. DOI: 10.17775/CSEEJPES.2021.08670.

Appendix

Results of rate of change of frequency ($RoCoF$) and frequency nadir (f_{nadir}) in Lanzarote-Fuerteventura power system when a sudden disconnection of the Diesel 9 generator unit of Punta Grande power plant takes place.

	Off-peak demand state												
	Conv case	Conv-wind case	Conv-wind-SC case H_{SC}= 2.0 MWs/MVA	Conv-wind-SC case H_{SC}= 2.5 MWs/MVA	Conv-wind-SC case H_{SC}= 3.0 MWs/MVA	Conv-wind-SC case H_{SC}= 3.5 MWs/MVA	Conv-wind-SC case H_{SC}= 4.0 MWs/MVA	Conv-wind-SC case H_{SC}= 4.5 MWs/MVA	Conv-wind-SC case H_{SC}= 5.0 MWs/MVA	Conv-wind-SC case H_{SC}= 5.5 MWs/MVA	Conv-wind-SC case H_{SC}= 6 MWs/MVA	Conv-wind-SC case H_{SC}= 6.5 MWs/MVA	Conv-wind-SC case H_{SC}= 7.0 MWs/MVA
$RoCoF$ (Hz/s)	-0.59	-0.76	-0.62	-0.60	-0.59	-0.57	-0.57	-0.56	-0.55	-0.55	-0.55	-0.54	-0.54
f_{nadir} (Hz)	49.42	49.36	49.41	49.41	49.42	49.43	49.43	49.44	49.45	49.45	49.46	49.46	49.47

	Peak demand state												
	Conv case	Conv-wind case	Conv-wind-SC case H_{SC}= 2.0 MWs/MVA	Conv-wind-SC case H_{SC}= 2.5 MWs/MVA	Conv-wind-SC case H_{SC}= 3.0 MWs/MVA	Conv-wind-SC case H_{SC}= 3.5 MWs/MVA	Conv-wind-SC case H_{SC}= 4.0 MWs/MVA	Conv-wind-SC case H_{SC}= 4.5 MWs/MVA	Conv-wind-SC case H_{SC}= 5.0 MWs/MVA	Conv-wind-SC case H_{SC}= 5.5 MWs/MVA	Conv-wind-SC case H_{SC}= 6 MWs/MVA	Conv-wind-SC case H_{SC}= 6.5 MWs/MVA	Conv-wind-SC case H_{SC}= 7.0 MWs/MVA
$RoCoF$ (Hz/s)	-0.35	-0.44	-0.39	-0.38	-0.37	-0.36	-0.36	-0.36	-0.36	-0.35	-0.35	-0.35	-0.35
f_{nadir} (Hz)	49.71	49.59	49.61	49.61	49.61	49.62	49.62	49.62	49.62	49.63	49.63	49.63	49.63

Results of minimum voltage values (U_{min}) in 66 kV and 132 kV buses of the transmission network of the Lanzarote-Fuerteventura power system when a sudden disconnection of the Diesel 9 generator unit of Punta Grande power plant takes place (in pu).

	Off-peak demand state												
	Conv case	Conv-wind case	Conv-wind-SC case H_{SC}= 2.0 MWs/MVA	Conv-wind-SC case H_{SC}= 2.5 MWs/MVA	Conv-wind-SC case H_{SC}= 3.0 MWs/MVA	Conv-wind-SC case H_{SC}= 3.5 MWs/MVA	Conv-wind-SC case H_{SC}= 4.0 MWs/MVA	Conv-wind-SC case H_{SC}= 4.5 MWs/MVA	Conv-wind-SC case H_{SC}= 5.0 MWs/MVA	Conv-wind-SC case H_{SC}= 5.5 MWs/MVA	Conv-wind-SC case H_{SC}= 6.0 MWs/MVA	Conv-wind-SC case H_{SC}= 6.5 MWs/MVA	Conv-wind-SC case H_{SC}= 7.0 MWs/MVA
Punta Grande 66 kV	0.981	0.979	0.990	0.990	0.991	0.991	0.991	0.991	0.991	0.991	0.991	0.991	0.991
San Bartolomé 66 kV	0.976	0.965	0.986	0.986	0.987	0.987	0.987	0.987	0.987	0.987	0.987	0.987	0.987
Mácher 66 kV	0.980	0.967	0.989	0.989	0.989	0.990	0.990	0.990	0.990	0.990	0.990	0.990	0.990
Playa Blanca 66 kV	0.991	0.962	1.000	1.000	1.000	1.000	1.000	1.000	1.000	1.001	1.001	1.001	1.001
Callejones 66 kV	0.976	0.965	0.986	0.986	0.987	0.987	0.987	0.987	0.987	0.987	0.987	0.987	0.987
Tías 66 kV	0.980	0.967	0.989	0.989	0.989	0.990	0.990	0.990	0.990	0.990	0.990	0.990	0.990
Las Salinas 66 kV	0.994	0.979	1.002	1.002	1.002	1.002	1.002	1.002	1.003	1.003	1.003	1.003	1.003
Corralejo 66 kV	0.992	0.963	1.001	1.002	1.002	1.002	1.002	1.002	1.002	1.002	1.002	1.002	1.002
Gran Tarajal 66 kV	0.991	0.956	0.999	1.000	1.000	1.000	1.000	1.000	1.000	1.000	1.001	1.001	1.001
Matas Blancas 66 kV	0.987	0.943	0.995	0.995	0.996	0.996	0.996	0.996	0.996	0.996	0.996	0.996	0.996
La Oliva 66 kV	0.993	0.965	1.002	1.002	1.002	1.002	1.002	1.002	1.003	1.003	1.003	1.003	1.003
Puerto Rosario 66 kV	0.994	0.978	1.002	1.002	1.002	1.002	1.002	1.003	1.003	1.003	1.003	1.003	1.003
Tías 132 kV	0.990	0.984	0.999	1.000	1.000	1.000	1.000	1.000	1.000	1.000	1.000	1.000	1.000
Playa Blanca 132 kV	0.991	0.985	1.000	1.000	1.001	1.001	1.001	1.001	1.001	1.001	1.001	1.001	1.001
La Oliva 132 kV	0.993	0.986	1.001	1.002	1.002	1.002	1.002	1.002	1.002	1.002	1.002	1.002	1.002
Puerto Rosario 132 kV	0.995	0.988	1.003	1.003	1.003	1.003	1.003	1.003	1.003	1.004	1.004	1.004	1.004
Gran Tarajal 132 kV	0.993	0.986	1.001	1.002	1.002	1.002	1.002	1.002	1.002	1.002	1.003	1.003	1.003
Jares 132 kV	0.993	0.985	1.001	1.002	1.002	1.002	1.002	1.002	1.002	1.002	1.003	1.003	1.003
Cañada Barca 132 kV	0.991	0.984	1.000	1.000	1.000	1.001	1.001	1.001	1.001	1.001	1.001	1.001	1.001
Matas Blancas 132 kV	0.991	0.984	0.999	1.000	1.000	1.000	1.000	1.000	1.001	1.001	1.001	1.001	1.001

	Peak demand state												
	Conv case	Conv-wind case	Conv-wind-SC case H_{SC}= 2 MWs/MVA	Conv-wind-SC case H_{SC}= 2.5 MWs/MVA	Conv-wind-SC case H_{SC}= 3 MWs/MVA	Conv-wind-SC case H_{SC}= 3.5 MWs/MVA	Conv-wind-SC case H_{SC}= 4 MWs/MVA	Conv-wind-SC case H_{SC}= 4.5 MWs/MVA	Conv-wind-SC case H_{SC}= 5 MWs/MVA	Conv-wind-SC case H_{SC}= 5.5 MWs/MVA	Conv-wind-SC case H_{SC}= 6 MWs/MVA	Conv-wind-SC case H_{SC}= 6.5 MWs/MVA	Conv-wind-SC case H_{SC}= 7 MWs/MVA
Punta Grande 66 kV	1.002	0.979	0.994	0.994	0.994	0.995	0.995	0.995	0.995	0.995	0.995	0.995	0.995
San Bartolomé 66 kV	0.988	0.965	0.982	0.982	0.982	0.982	0.982	0.982	0.982	0.982	0.982	0.983	0.983
Mácher 66 kV	0.992	0.967	0.985	0.985	0.986	0.986	0.986	0.986	0.986	0.986	0.986	0.986	0.986
Playa Blanca 66 kV	0.993	0.962	0.987	0.987	0.987	0.987	0.987	0.987	0.987	0.988	0.988	0.988	0.988
Callejones 66 kV	0.988	0.965	0.982	0.982	0.982	0.982	0.982	0.982	0.982	0.982	0.983	0.983	0.983
Tías 66 kV	0.992	0.967	0.985	0.985	0.986	0.986	0.986	0.986	0.986	0.986	0.986	0.986	0.986
Las Salinas 66 kV	1.013	0.979	1.000	1.000	1.000	1.000	1.000	1.000	1.000	1.000	1.000	1.000	1.000
Corralejo 66 kV	0.995	0.963	0.989	0.989	0.989	0.989	0.989	0.989	0.989	0.989	0.989	0.989	0.989
Gran Tarajal 66 kV	0.989	0.956	0.985	0.985	0.986	0.986	0.986	0.986	0.986	0.986	0.986	0.986	0.986
Matas Blancas 66 kV	0.978	0.943	0.974	0.975	0.975	0.975	0.975	0.975	0.975	0.975	0.975	0.975	0.975
La Oliva 66 kV	0.996	0.965	0.990	0.990	0.990	0.990	0.990	0.990	0.990	0.990	0.990	0.990	0.990
Puerto Rosario 66 kV	1.012	0.978	0.999	0.999	1.000	1.000	1.000	1.000	1.000	1.000	1.000	1.000	1.000
Tías 132 kV	0.998	0.968	0.993	0.993	0.993	0.993	0.993	0.993	0.993	0.994	0.994	0.994	0.994
Playa Blanca 132 kV	0.998	0.968	0.992	0.992	0.993	0.993	0.993	0.993	0.993	0.993	0.993	0.993	0.993
La Oliva 132 kV	1.000	0.968	0.993	0.993	0.994	0.994	0.994	0.994	0.994	0.994	0.994	0.994	0.994
Puerto Rosario 132 kV	1.003	0.971	0.995	0.996	0.996	0.996	0.996	0.996	0.996	0.996	0.996	0.996	0.996
Gran Tarajal 132 kV	0.994	0.960	0.990	0.990	0.990	0.990	0.990	0.990	0.990	0.990	0.990	0.990	0.991
Jares 132 kV	0.992	0.958	0.990	0.990	0.990	0.990	0.990	0.990	0.990	0.990	0.990	0.991	0.991
Cañada Barca 132 kV	0.989	0.954	0.985	0.985	0.986	0.986	0.986	0.986	0.986	0.986	0.986	0.986	0.986
Matas Blancas 132 kV	0.988	0.954	0.984	0.985	0.985	0.985	0.985	0.985	0.985	0.985	0.985	0.985	0.985